

Modelling of Supersonic and Subsonic Flows Using Hybrid Pressure-Based Solver in Openfoam

Janhavi Gharate¹, Rudra N. Roy²

^{1,2}Indian Institute of Technology, Goa
Farmagudi, Ponda-403401, Goa, India
janhavi1916303@iitgoa.ac.in; rudra@iitgoa.ac.in

Abstract - In this paper, validation of the hybrid central solver based on PIMPLE algorithm and KT scheme (*rhoPimpleCentralFoam*-solver) for high and low speed flows has been presented. Two different test cases were considered for the present study; a supersonic flow over a backward facing step with Mach number 2 and non-reacting subsonic flow separated by a bluff body with a Mach number 0.18. Backward facing step test case was studied using SST $k-\omega$ turbulence model, whereas performance of three different RANS based turbulence models, i.e. SST $k-\omega$ model, standard $k-\varepsilon$ model and modified $k-\varepsilon$ models were assessed for the flow over a bluff body. Results obtained from hybrid central solver for backward facing step using SST $k-\omega$ turbulence model showed good agreement with the experimental data. The mean flow features such as expansion fan, recirculation zone, boundary layers, shear layer and reattachment shock were also captured accurately. Whereas, the performance of the modified $k-\varepsilon$ turbulence model was found to be better as compared to other turbulence models in the predictions of flow structure of flow over a bluff-body.

Keywords: KT/KNP scheme, Backward facing step, Bluff body flow, PIMPLE algorithm.

1. Introduction

In high-speed compressible flows, suitable numerical schemes are required which can capture discontinuities such as shocks and contact surfaces accurately without any spurious oscillations. Some of the existing numerical methods such as monotone upstream-centred schemes for conservation laws (MUSCL) [1], piecewise parabolic method (PPM) [2], essentially non-oscillatory (ENO) schemes [3], weighted ENO (WENO) schemes [3], advection upstream of splitting method (AUSM) scheme [4-5], AUSM+ scheme [6] and the Runge-Kutta Galerkin (RKDG) method [7] are effective in producing non-oscillatory solutions. However, these methods involve Riemann solvers, characteristic decomposition, and Jacobian evaluation makes them complex and difficult to implement in a collocated polyhedral framework.

To overcome these issues, a generalization of the Lax–Friedrichs scheme was proposed by Nessyahu–Tadmor [8]. This method involves second-order central difference scheme, which provides higher resolution compared to Lax-Friedrichs scheme, and it also resolves the issue of excessive numerical dissipation up to some extent, but this scheme does not overcome the disadvantages of using smaller time step [8]. Further, explicit Kurganov-Tadmor (KT) scheme and Kurganov-Noelle-Petrova scheme (KNP) were developed and have been implemented in OpenFOAM in *rhoCentralFoam*-solver [9-10]. However, it was found that explicit KT/KNP schemes were not suitable for the low Mach number flows as even using very small-time step, it does not satisfy Courant criteria and converged solution cannot be obtained [8-11]. To overcome this difficulty, Kraposhin et al. [12] developed an approach by combining the KT/KNP scheme and the PISO method. In this method, the advection quantity was handled using KT/KNP fluxes, whereas the PISO algorithm was used to link pressure, energy and velocity. The scheme was developed in the OpenFOAM framework and named as *pisoCentralFoam*-solver and can be used to study compressible flows for a wide range of Mach numbers. However, it was found for large CFL values (> 0.1) PISO algorithm resulted in the underestimation of the characteristics speed of high-speed flows, i.e. resulted in the slight shift of the shock front or rarefaction wave. Further, these issues were mitigated by implementing a hybrid approach by combining PISO and SIMPLE algorithm known as PIMPLE algorithm [13] and the solver was named as *rhoPimpleCentralFoam*-solver. The above numerical scheme needs to be validated for low- and high-speed flows such that the scheme may be used to study both high-speed and low-speed reacting flows arising in practical combustors.

Hence, the objective of this study is to assess the performance of the hybrid scheme for wide ranges of Mach number. Initially, supersonic flow over a backward facing step will be used for assessing the performance of the hybrid scheme. This

test case comprises of flow near discontinuities and separation-attachment conditions. In the second case, non-reacting subsonic flow separated by a bluff-body will be used for the validation study. It comprises of a recirculation zone downstream of the bluff-body which enhances mixing of two fluids having same density.

2. Numerical Details

In this section, details about the governing equations, turbulence models and numerical schemes are provided. The governing equations for continuity, momentum, and energy transport are given as [14],

$$\text{Continuity equation} \quad \frac{\partial \bar{\rho}}{\partial t} + \frac{\partial \bar{\rho} \tilde{u}_i}{\partial x_i} = 0 \quad (1)$$

$$\text{Momentum equation} \quad \frac{\partial(\bar{\rho} \tilde{u}_i)}{\partial t} + \frac{\partial}{\partial x_j} \left[\bar{\rho} \tilde{u}_i \tilde{u}_j + \bar{p} \delta_{ij} + \overline{\rho u_i'' u_j''} - \bar{\tau}_{ij} \right] = 0 \quad (2)$$

$$\text{Energy equation} \quad \frac{\partial(\bar{\rho} \tilde{E})}{\partial t} + \frac{\partial}{\partial x_j} \left[\bar{\rho} \tilde{u}_j \tilde{E} + \tilde{u}_j \bar{p} + \overline{u_j'' p} + \overline{\rho u_i'' E''} + \bar{q}_j - \overline{u_i \tau_{ij}} \right] = 0 \quad (3)$$

In Eqs. (1-3) overbar refers to averaging through Reynolds decomposition, and tilde indicates density-weighted averaging. ρ is the density, t is the time, \mathbf{u} is the velocity vector, x_i is the special coordinate, p is the pressure, δ_{ij} is the Kronecker delta and q is the heat flux. The shear stress (τ_{ij}) and total energy (E) were estimated as given in ref. [15].

The term $-\overline{\rho u_i'' u_j''}$ appearing in Eq. (2) were closed using RANS based two-equation models. In the present study, $k-\epsilon$ [16] and SST $k-\omega$ [17] turbulence models were used. In this work hybrid pressure-based solver which combines PIMPLE algorithm with the KT scheme (rhoPimpleCentralFoam-solver) [13] was used. This algorithm relates the change in the pressure field with a change in the velocity field and density field using discretized pressure equation [12-13]. This solver uses switching function or blending function, which allows the solver to switch between the compressible and incompressible formulation of fluxes. This switching function K_f is dependent on the local Mach number and local acoustic Courant number which is given by,

$$K_f = \min \left(\frac{M_f}{A_{CFL}}, 1 \right) \quad (4)$$

Where, $M_f = \frac{u_f}{a_f}$ is the local Mach number at cell face, $A_{CFL} = a_f \frac{\Delta x}{\Delta t}$ is the local acoustic courant number and a_f is the speed

of sound at cell face. When the switching function tends to 1, the solver will use the compressible formulation of fluxes along with the PIMPLE algorithm, and when switching functions approaches zero, incompressible formulations of fluxes along the PIMPLE algorithm will be used.

3. Computational Details

In this section, computational details for the supersonic flow over a backward facing step and non-reacting subsonic bluff body flow are given.

3.1. Backward Facing Step

The experimental data obtained by McDaniel et al. [18] for supersonic flow over a backward facing step was used to validate the hybrid central scheme. The schematic of the backward facing step is shown in Fig. 2. The free stream velocity, static temperature and static pressure are 520 m/s, 167 K and 35 kPa, respectively [15, 19-20]. The free stream Mach number is 2, whereas the Reynolds number is 1.024×10^5 . A 2-D computational domain was selected to perform RANS calculations using *rhoPimpleCentralFoam*-solver. Uniform velocity boundary conditions were used at the inlet. For the top and bottom boundaries, no-slip and zero pressure gradient boundary conditions were used. SST $k-\omega$ (SST K-O) turbulence model was

used to model the turbulence. At the outlet faces, zero gradient boundary condition were given. Based on the grid independence study, 180×150 grids were selected. The results obtained are discussed in the subsequent section.

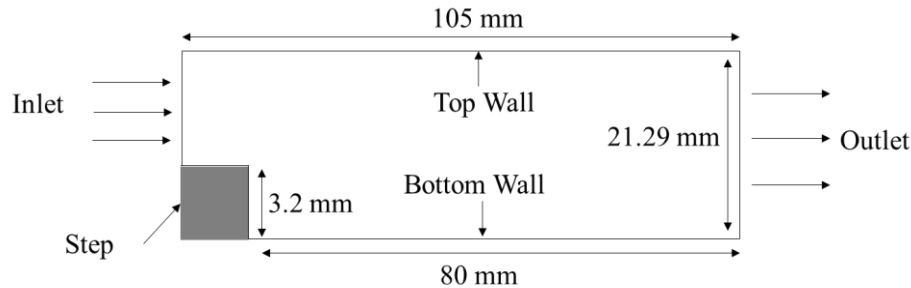


Fig. 2: Schematic of Backward facing step

3.2. Bluff Body Burner

The experimental data obtained by Masri et al. [21] for the non-reacting subsonic flow over bluff-body was used for the modelling purpose. The burner is centred in a coflowing stream of air and it consists of a circular bluff-body with an orifice at the centre for the main fuel to enter. The diameter of the bluff-body (D_b) is 50 mm, and that of the fuel jet is 3.6 mm. The bulk velocity of the fuel jet is 61 m/s, and the co-flowing air is 20 m/s. In this study, fuel jet comprises of air. The schematic of the bluff-body burner is shown in Fig. 2. Inlet static pressure is 1 bar, and inlet static temperature is 298 K. The free stream Mach number is 0.18, whereas Reynolds number is 14166. A 2-D computational domain was selected to study non-reacting bluff body flow with three different turbulence models, i.e. SST $k-\omega$ model (SST K-O), standard $k-\varepsilon$ model (SKE) and modified $k-\varepsilon$ model (MKE) using *rhoPimpleCentralFoam*-solver. In the MKE model, the value of the modelling constant $C_{\varepsilon 1}$ is modified from 1.44 to 1.6 in order to compensate for excessive diffusion [22, 23]. Uniform velocity boundary conditions were provided for both air and co-flow inlets. Uniform pressure boundary condition was given for the outlet boundary. The number of control volume selected were 120×100 based on the grid independence study.

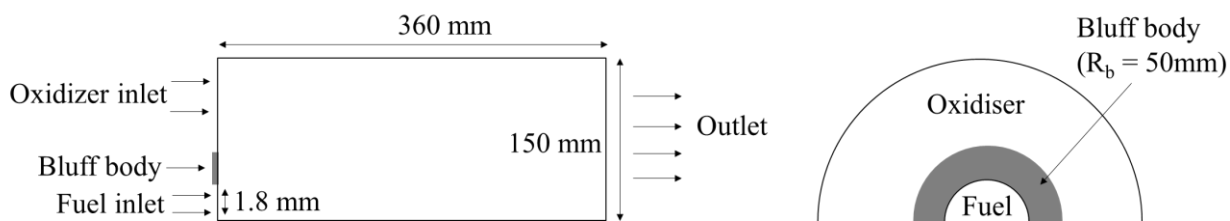


Fig. 3: Schematic of Bluff body burner

4. Result & Discussion

In this section, results obtained for the supersonic flow over a backward facing step and non-reacting subsonic bluff body flow are discussed.

4.1. Backward Facing Step

Figures 4, 5 and 6 show the predicted normalized radial pressure, velocity, and temperature profiles respectively at three different locations $x/h = 1.75$, 3 and 6.66. Axial location $x/h = 1.75$ is in the recirculation zone, reattachment region lies at $x/h = 3$, whereas $x/h = 6.66$ is at the downstream of the reattachment shock. It can be noticed from the normalized pressure profile shown in Fig 4, that initially, pressure decreases; after that, it increases as a reattachment shock wave is formed. Above the step, pressure increases monotonically in the radial direction across the expansion fan. After the expansion fan pressure is almost constant. From the normalized velocity profile shown in Fig. 5, it is clearly visible that near reattachment shock velocity increases radically, after the expansion fan velocity is nearly constant and near the top wall velocity decreases. From normalized temperature profile as shown in Fig. 6, it can be inferred that up to step height, there is a gradual decrease

in the temperature due to formation of reattachment shock, above the step temperature increases up to freestream temperature and after the expansion fan temperature remains constant but there is a slight decrease in temperature near the top wall. Results obtained from the simulation using rhoPimpleCentralFoam-solver agreed well with the experimental data except region near the step, i.e., $y/h < 1$ region because of the poor performance of RANS based turbulence models in the separation reattachment region.

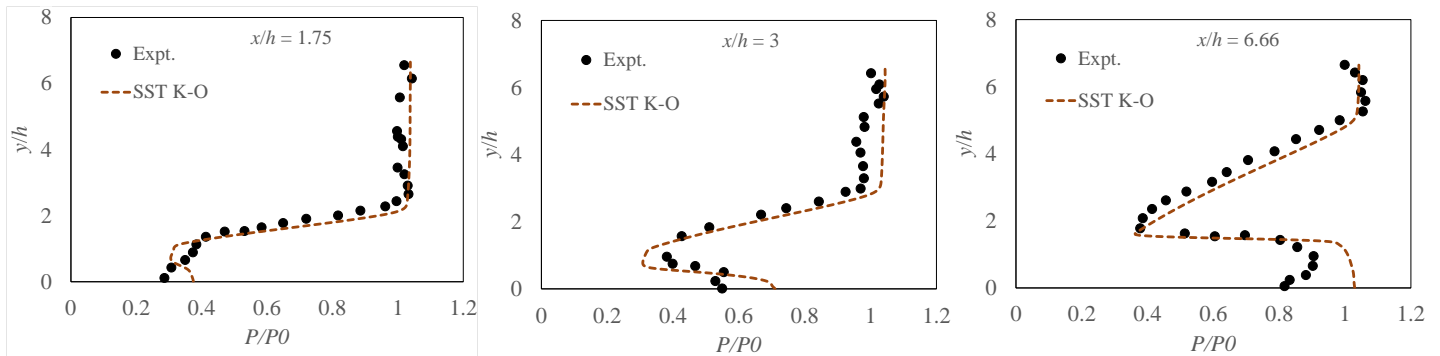


Fig. 4: Normalized radial pressure profiles at three different locations ($x/h = 1.75, 3$ and 6.66)

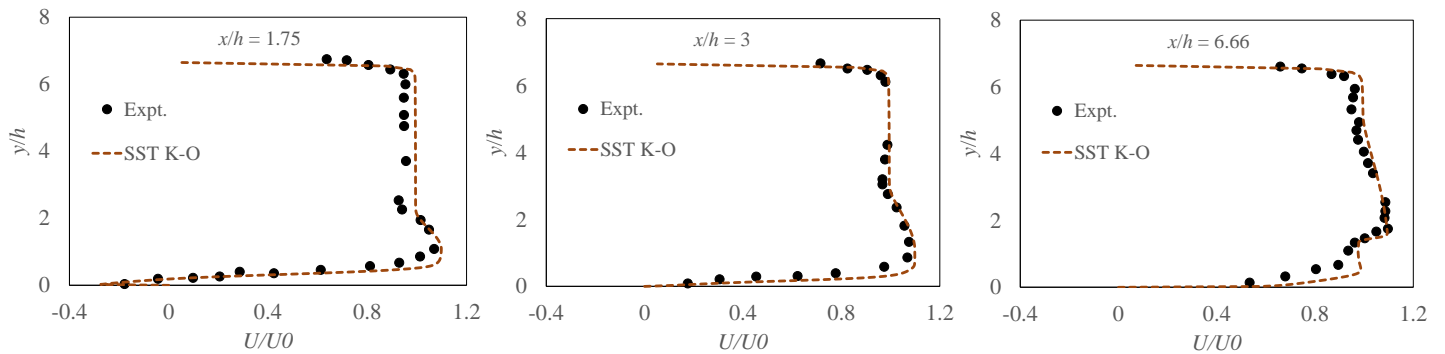


Fig. 5: Normalized radial velocity profiles at three different locations ($x/h = 1.75, 3$ and 6.66)

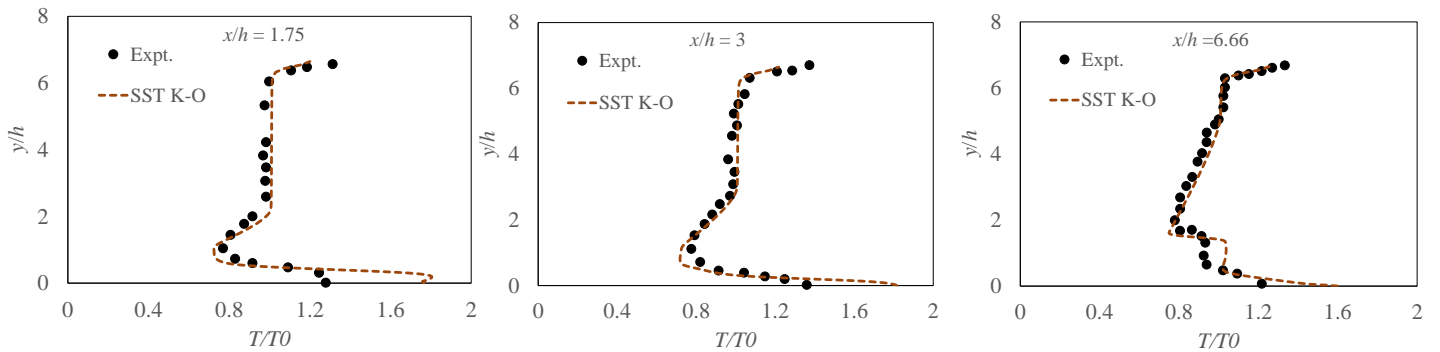


Fig. 6: Normalized radial temperature profiles at three different locations ($x/h = 1.75, 3$ and 6.66)

Figure 7 shows the pressure and velocity contours obtained from the RANS calculations. Mean flow features such as expansion fan, boundary layer, recirculation zone, shear layer and reattachment shock have been captured well as shown in Fig. 7. Expansion fan is created at the step corner due to sudden turning of a flow around a convex edge, further gradual reduction in pressure across the expansion fan can be observed. Behind the step, small subsonic recirculation

zone is formed. Pressure in the recirculation zone is less as compared to that in the downstream locations. The shear layer is generated from the separation of boundary layers. This shear layer gets compressed in the further downstream direction, and reattachment shock is formed at the lower wall. Velocity and pressure contours in Fig. 7 depict the formation of recirculation zone, shear layer and reattachment shock.

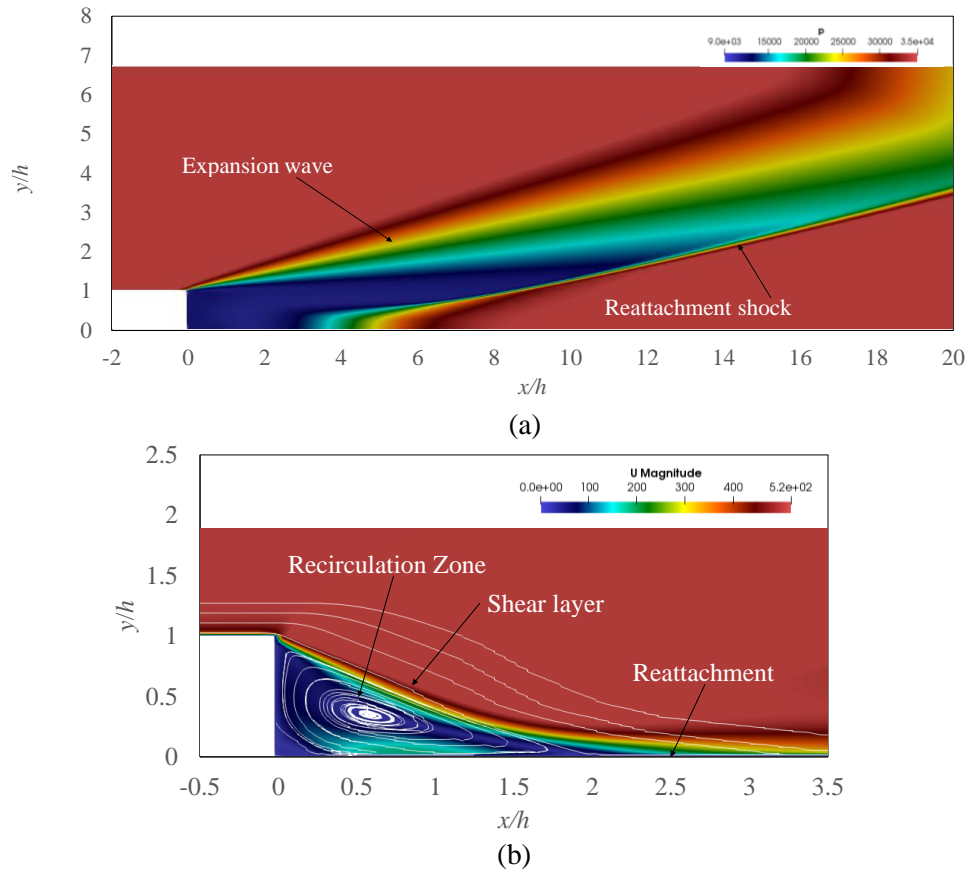


Fig. 7: (a) Pressure field and (b) Velocity field

4.2. Bluff Body Burner

Figures 8 and 9 shows the predicted radial velocity by three different turbulence models, i.e., SST K-O, SKE and MKE models. Six different axial locations were selected to compare the predicted velocity field with experimental data. Axial locations $x/D_b = 0.2$ to 0.8 are in the recirculation region, and the predicted velocity fields are shown in Fig. 8. It can be observed from Fig. 8 that the predicted velocity by the SST K-O model at the upstream locations, i.e., at $x/D_b = 0.2$ and 0.4 agreed very well with the experimental data. However, at downstream locations, i.e., at $x/D_b = 0.6$ and 0.8 , SST K-O model overpredicts the velocity profile from $0.2 < r/r_b < 0.9$ and underpredicts the velocity distribution significantly near the centre, i.e., $r/r_b < 0.2$ as SST K-O model is less sensitive to the free stream region. A similar trend for predictions was also obtained from the SKE model. However, the predicted velocity field by the MKE model agreed very well with the experimental data, as shown in Fig. 8.

Axial locations, i.e. $x/D_b = 1$ and 1.3 , are immediately downstream of the recirculation zone, and the predicted radial velocity distribution for these locations are shown in Fig. 9. It can be observed from the Fig. 9 that SST K-O and SKE model underpredict the velocity distribution near the centre, i.e., $r/r_b < 0.2$ for axial locations $x/D_b = 1$ and 1.3 and overpredict the result in the region from $0.2 < r/r_b < 0.6$ for axial location $x/D_b = 1$. Whereas velocity profile predicted using MKE model agrees with the experimental data with reasonable accuracy.

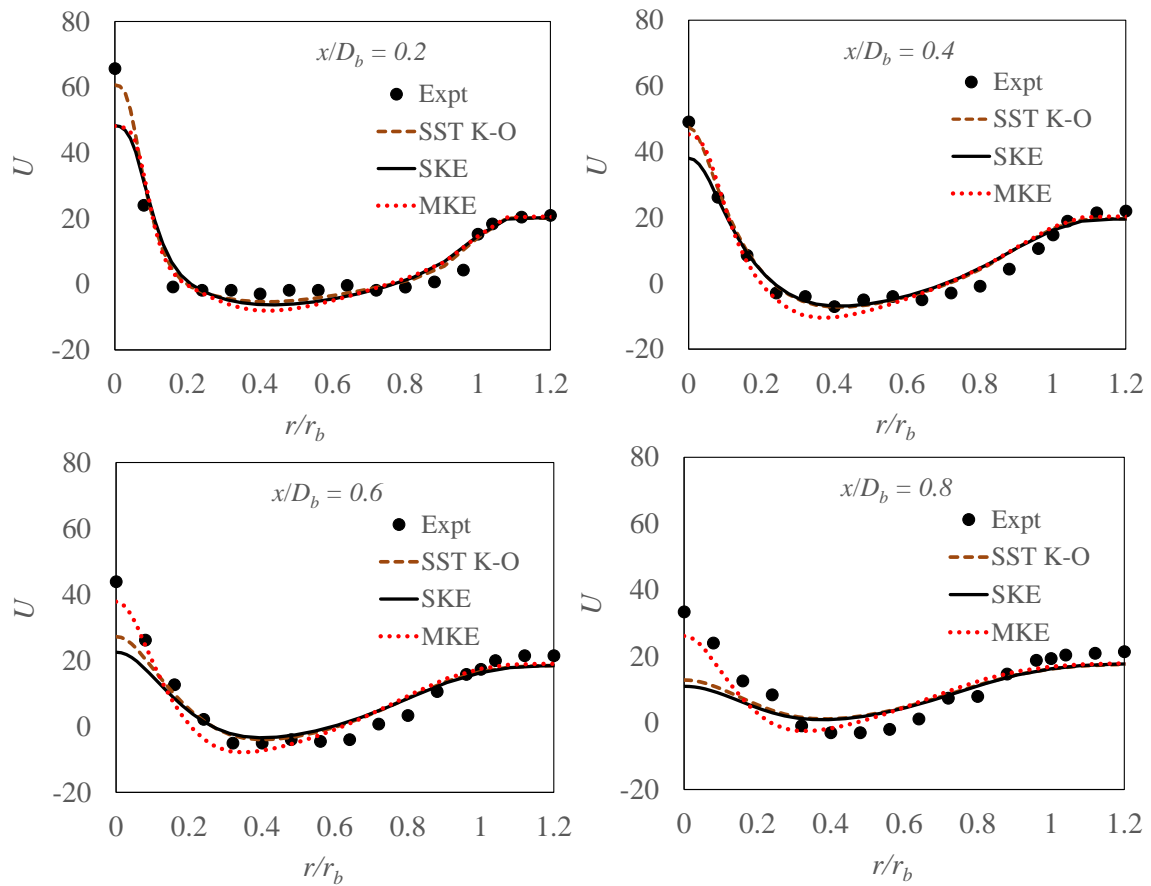


Fig. 8: Comparison of predicted radial velocity with the experimental data at four different axial locations ($x/D_b = 0.2, 0.4, 0.6$ and 0.8)

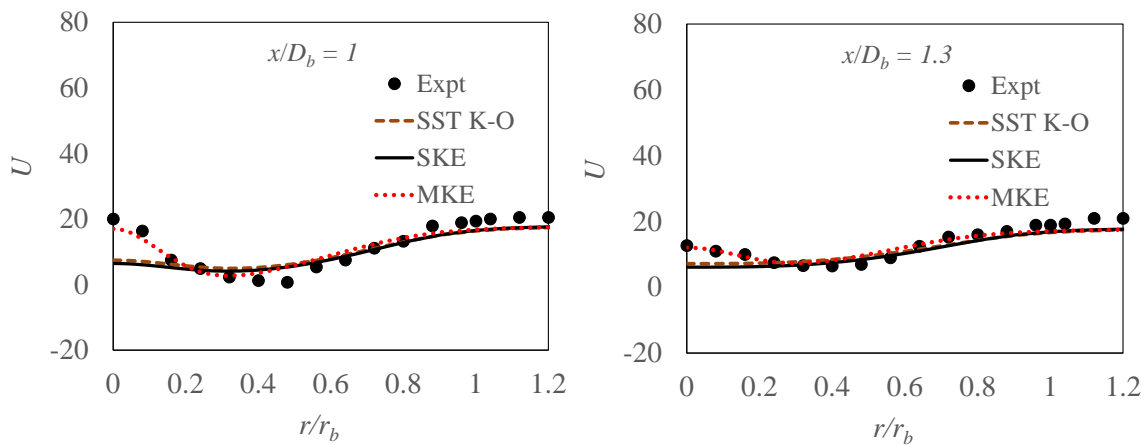


Fig. 9: Comparison of predicted radial velocity with the experimental data at two different axial locations ($x/D_b = 1$ and 1.3)

Figure 10 shows the velocity contour predicted by the MKE model. A low-pressure area is formed near the bluff body; fuel and oxidizer streams flow backwards towards that area, creating a recirculation zone. The streamlines structures in Fig. 10 two counter-rotating vortices that may enhance the mixing of fuel and oxidizer.

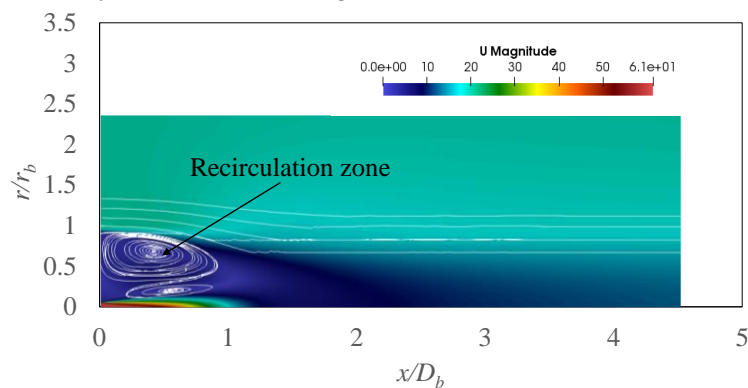


Figure 10. Predicted velocity field by MKE model

5. Conclusion

In this paper, a hybrid solver available in OpenFOAM was validated against turbulent supersonic flow over a backward facing step and non-reacting subsonic bluff body flow. For the backward facing step, numerical results obtained using the SST $k-\omega$ turbulence model with *rhoPimpleCentralFoam*-solver agreed with the experimental data with reasonable accuracy except in the region $y/h < 1$ as RANS based turbulence models fails to predict flow separation accurately. Mean flow features such as expansion fan, boundary layers, shear layer, recirculation zone and reattachment shock were captured accurately.

For the non-reacting subsonic bluff body flow, the velocity field was obtained using *rhoPimpleCentralFoam*-solver. Three different RANS based turbulence models, i.e. SST $k-\omega$, standard $k-\epsilon$ and modified $k-\epsilon$ were used to predict the velocity field. It was observed that the modified $k-\epsilon$ turbulence model provides more accurate results as compared to the SST $k-\omega$ model and standard $k-\epsilon$ model. The validated flow solver may further be used to predict the flame structure arising in high and low speeds reacting flows.

Acknowledgements

The authors are grateful to the Indian Institute of Technology Goa for funding this research work.

References

- [1] S. I. Sohn, "A new TVD-MUSCL scheme for hyperbolic conservation laws," *Comput. Math. Appl.*, vol. 50, pp. 231-248, 2005.
- [2] P. Colella, P. R. Woodward, "The piecewise parabolic method (PPM) for gas-dynamics simulations," *J. Comput. Phys.*, vol. 54, no. 1, pp. 174-201, 1984.
- [3] Y. T. Zhang, C. W. Shu, "ENO and WENO schemes," *Handbook Numer. Analy.*, vol. 17, pp. 103-122, 2016.
- [4] M. Hajzman, O. Bublik, J. Vimmr, "On the modelling of compressible inviscid flow problems using AUSM schemes," *Appl. Comput. Mech.*, vol. 1, pp. 469-478, 2007.
- [5] M. S. Liou, "Evolution of Advection Upstream Splitting Method Schemes," *Def. Sci. J.*, vol. 60, no. 6, pp. 606-613, 2010.
- [6] M. S. Liou, "A sequel to AUSM: AUSM+," *J. Comput. Phys.*, vol. 129, no. 2, pp. 364-382, 1996.
- [7] C. W. Shu, "Runge-Kutta discontinuous Galerkin methods for convection dominated problems," *J. Sci. Comput.*, vol. 16, no. 3, pp. 173-261, 2001.

- [8] H. Nessyahu, E. Tadmor, "Non-oscillatory central differencing for hyperbolic conservation laws," *J. Comput. Phys.*, vol. 87, pp. 408–447, 1990.
- [9] A. Kurganov, E. Tadmor, "New High-Resolution Central Schemes for Nonlinear Conservation Laws and Convection Diffusion Equations," *J. Comput. Phys.*, 160, pp. 241–282, 2000.
- [10] A. Kurganov, S. Noelle, G. Petrova, "Semi-discrete central-upwind schemes for hyperbolic conservation laws and Hamilton–Jacobi equations," *SIAM J. Sci. Comput.*, vol. 23, pp. 707–740, 2001.
- [11] M. S. Liou, C. J. Steffen Jr, "A new flux splitting scheme," *J. Comput. Phys.*, vol. 107, no. 1, pp. 23–39, 1993.
- [12] M. Kraposhin, A. Bovtrikova, S. Strijhak, "Adaptation of Kurganov-Tadmor numerical scheme for applying in combination with the PISO method in numerical simulation of flows in a wide range of Mach numbers," *Procedia Comp. Sci.*, vol. 66, pp. 43-52, 2015.
- [13] M. Kraposhin, M. Banholzer, M. Pfitzner, I. K. Marchevsky, "A hybrid pressure-based solver for nonideal single-phase fluid flows at all speeds," *Int. J. Num. Methods Fluids*, vol. 88, pp. 79–99, 2018.
- [14] H. K. Versteeg, W. Malalasekera, *Introduction to computational fluid dynamics*. Pearson Education Limited: 2nd Ed., 2007.
- [15] R. K. Soni, N. Arya, A. De, "Assessment of RANS based models in a supersonic flow," *American Institute of Physics: Conference Proceedings 1648*, 2015, pp. 030039-1–030039-4.
- [16] B. E. Launder, D. B. Spalding, "The numerical computation of turbulent flows," *Comp. Methods Appl. Mecha. Eng.*, vol. 3, pp. 269–289, 1974.
- [17] F. R. Menter, "Two-Equation Eddy-Viscosity Turbulence Models for Engineering Applications," *AIAA J.*, vol. 32, pp. 1598–1605, 1994.
- [18] J. C. McDaniel, D. G. Fletcher, R. J. Hartfield, "Staged transverse injection into Mach 2 flow behind a rearward-facing-step: a 3D compressible flow test case for hypersonic combustor CFD validation," *AIAA Paper*, 1992.
- [19] R. K. Soni, N. Arya, A. De, "Numerical simulation of supersonic separating-reattaching flow through RANS," *J. Phys.: Conf. Series 822*, 2017.
- [20] R. K. Soni, N. Arya, A. De, "Characterization of turbulent supersonic flow over a backward-facing step," *AIAA J.*, vol. 55, pp. 1511-1529, 2017.
- [21] A. R. Masri, R. W. Bilger (1999). Bluff body flows and flames, The University of Sydney, clean combustion research group [Online]. Available: <https://web.aeromech.usyd.edu.au/thermofluids/bluff.php>
- [22] R. N. Roy, S. Sreedhara, "A numerical study on the influence of airstream dilution and jet velocity on NO emission characteristics of CH₄ and DME bluff-body flame," *Fuel*, vol. 142, pp 73-80, 2015.
- [23] R. N. Roy, S. Sreedhara, "Modelling of methanol and H₂/CO bluff-body flames using RANS based turbulence models with conditional moment closure model," *Appl. Therm. Eng.*, vol. 93, pp. 561-570, 2016.